

Phase diagram of aggregation of oppositely charged colloids in salty water

R. Zhang and B. I. Shklovskii

Theoretical Physics Institute, University of Minnesota, Minneapolis, Minnesota 55455

(Dated: March 22, 2024)

Aggregation of two oppositely charged colloids in salty water is studied. We focus on the role of Coulomb interaction in strongly asymmetric systems in which the charge and size of one colloid is much larger than the other one. In the solution, each large colloid (macroion) attracts certain number of oppositely charged small colloids (Z-ion) to form a complex. If the concentration ratio of the two colloids is such that complexes are not strongly charged, they condense in a macroscopic aggregate. As a result, the phase diagram in a plane of concentrations of two colloids consists of an aggregation domain sandwiched between two domains of stable solutions of complexes. The aggregation domain has a central part of total aggregation and two wings corresponding to partial aggregation. A quantitative theory of the phase diagram in the presence of monovalent salt is developed. It is shown that as the Debye-Huckel screening radius r_s decreases, the aggregation domain grows, but the relative size of the partial aggregation domains becomes much smaller. As an important application of the theory, we consider solutions of long double-helix DNA with strongly charged positive spheres (artificial chromatin). We also consider implications of our theory for in vitro experiments with the natural chromatin. Finally, the effect of different shapes of macroions on the phase diagram is discussed.

PACS numbers: 61.25.Hg, 82.70.Dd, 87.14.Gg, 87.15.Nn

I. INTRODUCTION

Aggregation or self-assembly of oppositely charged colloids is a general phenomenon in biology, pharmacology, and chemical engineering. The most famous biological example is the chromatin made of long negatively charged double-helix DNA and positively charged histone octamers¹. Due to Coulomb interaction, DNA winds around many octamers to form a beads-on-a-string structure, also called 10 nm fiber (see Fig. 1 for an illustration). This 10 nm fiber may self-assemble into a 30 nm fiber, which is the major building material of a chromosome. The formation of 30 nm fiber strongly depends on the concentration of salt in the solution. This means that the Coulomb interaction plays a crucial role². The best known pharmacological example is the problem of gene therapy. In this case, a negatively charged DNA helix should penetrate through a negatively charged cell membrane. To do this, DNA has to be neutralized or overcharged by complexation with positive polyelectrolytes or colloids. At the same time aggregation of these complexes can be useful or should be avoided^{3,4,5,6,7,8,9}. Industrial examples of aggregation include using cationic polyelectrolyte as coagulants for paper manufacturing, mineral separation, and the aggregation-induced removal of particulate matter from the aqueous phase in water and wastewater treatment processes¹⁰. Given such wide applications, it is therefore interesting to construct a general physical theory on aggregation of oppositely charged colloids.

In this paper, we consider the equilibrium state of two kinds of oppositely charged colloids in salty water and construct the phase diagram of such a system. Without losing generality, we call the larger colloid "macroion" with negative charge $-Q$, concentration

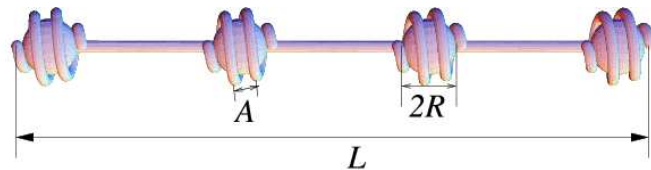


FIG. 1: A beads-on-a-string structure of the complex of a long negative polymer macroion with positive spherical Z-ions (artificial chromatin).

p , and the smaller colloid "Z-ion" with positive charge Ze (e is the proton charge), concentration s . Macroions can be big spheres (big colloid particles), rigid cylinders (short DNA) or long semi-flexible polymers (long DNA). Z-ions can be small spheres (nucleosome core particles, micelles or dendrimers) or short polymers (polyamines). Most of such systems are strongly asymmetric in the sense that the size and charge of the macroion are much larger than those of the Z-ion (Figs. 1, 2, 3). Therefore, denoting the number of Z-ions neutralizing one macroion as $N_i = Q/Ze$ (the subscript i denoting "isoelectric"), we focus on systems with $N_i \gg 1$.

In the previous paper¹¹ this problem was considered for long semi-flexible polymers (DNA double helices) as macroions and rigid synthetic spheres with very large charge as Z-ions (Fig. 1) without monovalent salt. In such a system each polymer macroion winds around a number of spherical Z-ions and forms a periodic necklace-like structure which is similar to the natural chromatin. We call it "artificial chromatin". The phase diagram Fig. 4a was obtained in a plane of the macroion (DNA) concentration, p , and the Z-ion (spheres) concentration, s (notations s and p are introduced as abbreviation for

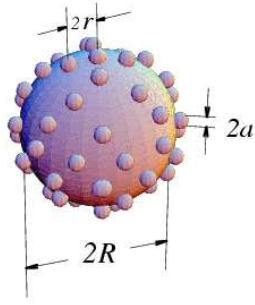


FIG. 2: A complex of a negative spherical macroion with positive spherical Z-ions condensing on it.

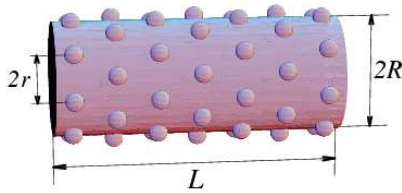


FIG. 3: A complex of a negative cylindrical macroion with positive spherical Z-ions condensing on it. Z-ions form 2D Wigner-crystal-like liquid on the surface of the macroion.

"sphere" and "polymer"). As seen from Fig. 4a, around the line of neutrality (the dashed line) where macroion-Z-ions complexes are almost neutral, they condense in a macroscopic aggregate (the gray region). Far away from this line, the complexes are strongly charged and they stay free in the solution (the white region).

It should be emphasized that strong correlations play a crucial role in the origin of this picture. First, spherical Z-ions in the necklace repel each other to form a 1D liquid with almost periodic structure similar to one-dimensional Wigner crystal (see Fig. 1). This leads to a correlation energy gain in addition to the mean field Coulomb energy of the spheres. The difference between this gain and the entropic gain in the bulk per Z-ion plays the role of a voltage which may overcharge necklaces (making them positive). As a result, a free macroion-Z-ions complex can be either positive (above the dashed line in Fig. 4a) or negative (below the dashed line in Fig. 4a) depending on concentrations s and p . Second, the polymer turns wound around a spherical Z-ion repel each other and form an almost equidistant coil. This correlation orders a short-range attraction between complexes as illustrated by Fig. 5. When complexes are almost neutral, this attraction is able to condense them. When they are strongly charged, Coulomb repulsion is larger than the short-range attraction and they stay free.

An important feature of Fig. 4a is two relatively wide domains, where aggregation of macroion-Z-ions com-

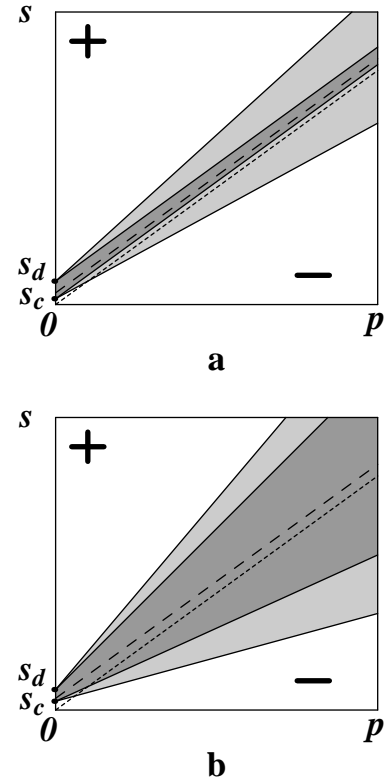


FIG. 4: Phase diagrams of the artificial chromatin system. a: without monovalent salt. b: with monovalent salt. (Spherical and cylindrical macroion systems have similar phase diagrams with a much larger s_d .) p is the concentration of macroions (DNA), s is the concentration of Z-ions (spheres). Plus and minus are the signs of the charge of free macroion-Z-ions complexes. The dark gray region is the domain of total aggregation of complexes, while the light gray region is the domain of their partial aggregation. The white region is the domain of free complexes. s_c and s_d are concentrations of Z-ions at the boundary of the aggregation domain when $p \neq 0$. At the dotted "isoelectric" line the absolute values of the total charges of macroions and Z-ions in the solution are equal. At the dashed "neutrality" line free complexes are neutral.

plexes is only partial (the light gray region). This means that certain fraction of complexes aggregates, while others stay free in the solution. The reason for partial aggregation is redistribution of Z-ions between aggregated and free complexes. When (p, s) is such that the Coulomb repulsion between complexes is slightly larger than the short-range attraction, Z-ions can redistribute themselves so that for a fraction of complexes the Coulomb repulsion becomes substantially smaller and they aggregate, while for the rest of complexes the Coulomb repulsion becomes even larger and they stay free¹². Without monovalent salt, the macroscopic aggregate should be practically neutral (a net charge defined as the sum of charges of the macroion and Z-ions should be close to zero). As a result, the domain of total aggregation is

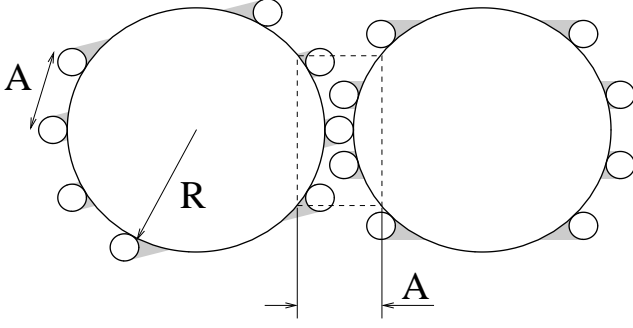


FIG. 5: Cross section through the centers of two touching positive spherical Z -ions with turns of negative semirigid polymers (gray) wound around them. At the place where two spheres touch each other (the rectangle), the density of polymer segments doubles and the correlation energy is gained.

narrow while the domain of partial aggregation is much wider (see Fig. 4a).

In this paper, we develop a general phenomenological theory of complexation and aggregation of oppositely charged macroions and Z -ions in the presence of monovalent salt. In order to formulate this theory we use the simplest model of spherical rigid macroions and small Z -ions shown in Fig. 2. In the absence of monovalent salt, the phase diagram of this system looks like Fig. 4a, where p is the concentration of spherical macroions and s is the concentration of Z -ions. Screening by monovalent salt effectively truncates the Coulomb interaction at the Debye-Hückel screening radius r_s . If r_s is smaller than the size of the spherical macroions, the Coulomb repulsion of two macroion- Z -ions complexes is almost completely screened even when they touch each other. Therefore, aggregation is possible even if macroion- Z -ions complexes carry a net charge (defined as the sum of charges of the macroion and Z -ions). As a result, screening strongly modifies the phase diagram as shown in Fig. 4b. Comparing with the phase diagram without monovalent salt (Fig. 4a), we see that the aggregation domain grows. At the same time, the relative size of the partial aggregation domain (the light gray region) in the whole aggregation domain decreases, because redistribution of Z -ions between aggregated and free complexes becomes less important.

Our phenomenological theory of Sec. II contains several parameters depending on charges, sizes, shapes and flexibility of macroions and Z -ions. In sections III, IV and V we evaluate microscopically these parameters for specific pairs of macroions and Z -ions. In Sec. III we do this for a system of spherical macroions and small Z -ions (Fig. 2) and find slopes of phase diagram boundaries in this case. In Sec. IV we repeat this calculation for cylindrical macroions (Fig. 3). In Sec. IV we return

to artificial chromatin (Fig. 1) and revise some results of Ref. 11 related to the screening effect of monovalent salt.

We find that although all these systems have phase diagrams similar to Fig. 4b, the width of aggregation domain and relative width of the partial aggregation domains depend on the pair. Namely, rigid cylindrical macroions have the largest aggregation domain, because parallel cylinders have relatively larger area where they can touch each other. Artificial chromatin (Fig. 1) on the other side has the smallest aggregation domain. This peculiarity will be explained in Sec. V. There we also show that phase diagram of Fig. 4b seems to agree with results of experiments in vitro designed to understand regulation of natural chromatin¹⁵.

II. PHENOMENOLOGICAL THEORY OF AGGREGATION IN THE PRESENCE OF MONOVALENT SALT

In this section we discuss the general theory of the phase diagram in the presence of monovalent salt using the system of spherical macroions shown in Fig. 2. Aggregation of two such spherical macroions is illustrated by Figs. 6 and 7. Z -ions form a strong correlated liquid on the surface of the macroion. The negative correlation energy in this liquid results in the voltage which may overcharge the complex. It also induces a short-range attraction between complexes since in the spot where two complexes touch each other (see Fig. 6) the surface density of the correlated liquid is doubled and the energy per Z -ion is reduced¹⁶. This attractive force decays as $\exp(-2d/3r)$ (for a triangular lattice)¹⁷ with the distance d between two surfaces, where r is the half of average distance between nearest neighbor Z -ions on the macroion surface, or, in other words, the radius of the Wigner-Seitz cell. Consequently, only a small disk-like contact region with radius $W = \frac{p}{3-2p} Rr$, where $p = \frac{3-2p}{3-2p} 0.3$, contributes to the attraction of two complexes (see Fig. 6). We call it "sticky region".

Similarly to artificial chromatin, this correlation attraction leads to phase diagram Fig. 4a in the absence of screening. We should remember, however, that in the case of Fig. 2, s stands for the concentration of small spherical Z -ions, and p is the concentration of large spherical macroions. We show below that screening not only enlarges the aggregation domains, but also leads to relatively smaller size of the partial aggregation domain. These effects become strong when r_s is smaller than R . They grow when r_s is reduced all the way to r and even at $r_s < r$. Only when r_s is so small that interaction of a Z -ion with macroion surface becomes smaller than $k_B T$, most of Z -ions leave the macroion surface, and aggregation becomes impossible. Below we concentrate on the case $r > r_s > R$ which can be described by simple and universal phenomenological theory.

There is a key difference between the cases without screening discussed in Ref. 11 and with screening effect

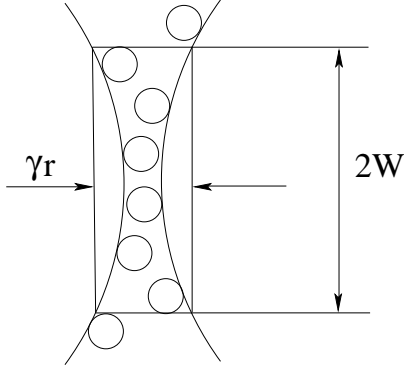


FIG. 6: The cross section of the touching area of two aggregated spherical macroions. The sticky region is shown by the rectangle. In this region, the density of Z -ions doubles and the correlation energy is gained.

of monovalent salt. In the first case, each macroion of the aggregate can only carry N_1 Z -ions, i.e., the aggregate is almost neutral. This is because if macroion- Z -ions complexes were charged, the Coulomb potential of the aggregate would increase with its size and become too large to continue aggregation. On the other hand, in the presence of strong screening by monovalent salt, when the local distance between the two touching surfaces, d , is much larger than r_s , the Coulomb interaction between two surfaces is exponentially small and can be neglected (see Fig. 7). It only affects the disk-like surface region with radius $W_s = \frac{1}{2}Rr_s$ located inside the cylinder where $d < 2r_s$. We refer to such a cylinder as " r_s -cylinder" (shown by the dashed rectangular in Fig. 7). Therefore, if we count only charges of macroions and Z -ions, the aggregate of macroion- Z -ions complexes need not be neutral. Most of the surface area of these complexes can be overcharged or undercharged in the same way as surfaces of free complexes.

We argue that macroion surface charge density, $\sigma(d)$ (including charge of the macroion and Z -ions), inside r_s -cylinder is much smaller than the one outside r_s -cylinder, σ_0 . In electrostatics, it is known that for two charged contacting metallic spheres in vacuum, the surface charge density goes to zero when we move to the point of contact (one can show that it decays as $\exp(-R/d)$). Our case is similar to this example in the sense that Z -ions equilibrate on macroion surfaces so that everywhere they acquire the same electrochemical potential, $\mu_c(N) + e\phi$. The chemical potential $\mu_c(N)$ determined by correlations of Z -ions depends on concentration of Z -ions on the surface of macroion, which, as shown below, can be regarded as a constant. This means that the electrostatic potential is a constant, too, similarly to the case of two metallic spheres. The peculiarity of our case is that the presence of monovalent salt which screens the surface electric potential. Deep inside r_s -cylinder, screening by monovalent salt is incomplete. Indeed, according to the Debye-Hückel

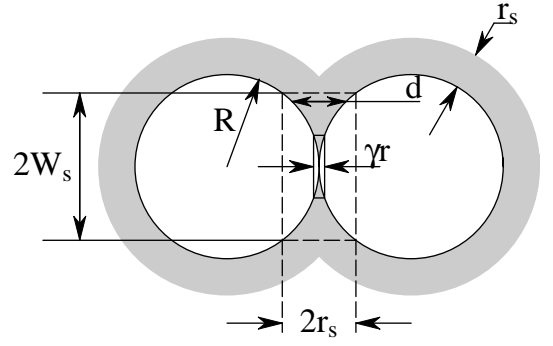


FIG. 7: The cross section of the two aggregated spherical macroions. Z -ions adsorbed on them are not shown. The width of the gray region is the effective range of the Coulomb interaction in the presence of monovalent salt. The neutral r_s -cylinder is shown by the rectangle of dashed lines. It is larger than the sticky region shown by the full line rectangle (see Fig. 6).

theory, the density of screening charge of monovalent salt near the macroion surface has the same magnitude $\sigma = -4\pi\epsilon_0\epsilon_r r_s$ as outside of r_s -cylinder. But with decreasing d , the volume occupied by this charge shrinks very fast. At $d = r_s$, charge density of monovalent salt projected to the macroion surface, $\sigma_0 = -4\pi\epsilon_0\epsilon_r r_s$, is much smaller than σ_0 . As we saw from the problem of two contacting metallic spheres, the total surface charge density between two touching spherical surfaces with constant potential decays very fast towards the contact point. Accordingly, inside the r_s -cylinder at $d = r_s$, the surface charge density $\sigma = -2\pi\epsilon_0\epsilon_r r_s$ is very small (it decays with decreasing d as $\sigma_0 \exp(-R/d)$). Therefore, for the surface charge density of the macroion $\sigma(d)$, we arrive at $\sigma(d) = \sigma_0(d) = -2\pi\epsilon_0\epsilon_r r_s$. Since at $d = r_s$, $\sigma(d)$ is much smaller than σ_0 , we call this region "neutral region". At $d = r_s$, the sticky region discussed above (the full line rectangle in Figs. 6 and 7) is much smaller than the neutral region and therefore almost neutral.

Let N be the number of Z -ions in a free macroion- Z -ions complex. We define $Q = Q + NZe = Ze(N - N_1)$ as the net charge of a free complex, and $(1 - \alpha)Q$ as the net charge of the aggregated complex. The total number of Z -ions in an aggregated complex is therefore $N - (N - N_1)$.

At $d = R$, the whole complex is neutral in the aggregate, so $\alpha = 1$. At $d = R$, away from neutral regions, due to equilibration of Z -ions, aggregated macroion- Z -ions complexes have the same surface density of Z -ions as free complexes. Thus, α is a measure of the fraction of total surface area of a complex occupied by neutral regions. α decreases with decreasing r_s .

Now we can write down the free energy of the system. Similarly to Ref. 11, we start from a point $(p; s)$ in the domain of partial aggregation and assume that a fraction x of aggregated macroion- Z -ions complexes. The free

energy per unit volume is

$$F(N; x; s; p) = (1-x)p \frac{Q^2}{2C} + N E(N) + xp \left((1-x) \frac{Q^2}{2C} + N E(N) - c(N - N_i) \right) + k_B T \left[s \left((1-x)pN - xp(N - (N - N_i)) \right) \right] \ln \frac{[s \left((1-x)pN - xp(N - (N - N_i)) \right)] v_0}{e} \quad (1)$$

The first line of Eq. (1) is the free energy density of free macroion-Z⁻ions complexes. It consists of Coulomb energy of complexes and correlation energy of Z⁻ions. Here C is the capacitance of a free complex, $E(N) < 0$ is the correlation energy per Z⁻ion in the complex. The second line of Eq. (1) is the free energy density of aggregated complexes. Here $c < 0$ is the additional correlation energy per complex due to aggregation¹⁸ and $c(N) = \theta(N E(N)) = \theta(N < 0)$ is the part of the chemical potential of Z⁻ions related to their correlations on the surface of a macroion. It has been assumed in Eq. (1) that $N - N_i = N_i$ (this will be confirmed later) and therefore

$$c(N) = c(N_i) = c \quad (2)$$

In the second line of Eq. (1) the first term is the Coulomb energy of an aggregated complex diminished by a loss of fraction of capacitor area, the second and third term give correlation energy of Z⁻ions diminished by loss of $(N - N_i)$ of them and the fourth term is responsible for attraction energy of aggregated complexes in sticky regions. The third and fourth line of Eq. (1) give the free energy density of free Z⁻ions related to their entropy, (v_0 is the normalizing volume). The entropy of macroions is ignored because of their much smaller concentration. Minimizing this free energy with respect to N and x , we get

$$c + \frac{ZeQ}{C} = k_B T \ln \left[(s - (1-x)pN - xp(N - (N - N_i))) v_0 \right]; \quad (3)$$

$$\frac{Q^2}{2C} = (N - N_i) f_c - k_B T \ln \left[(s - (1-x)pN - xp(N - (N - N_i))) v_0 \right]; \quad (4)$$

Excluding the entropy term from in Eqs. (3) and (4), we get

$$N_{cjd} = N_i - 1 - \frac{s \frac{j j 2C (r_s)}{(r_s) Q^2}}{Q^2}; \quad (5)$$

Here and below, the upper (lower) sign in the formula always corresponds to the first (second) subscript of the symbol.

Plugging Eq. (5) back to Eq. (3), we get

$$s_{cjd}(p) = s_{cjd} + (1-x)pN_{cjd} + xp[N_{cjd} - (c_s)(N_{cjd} - N_i)]; \quad (6)$$

where

$$s_{cjd} = \frac{1}{v_0} \exp \left[\frac{1}{k_B T} \frac{s \frac{j j 2C (r_s)}{(r_s) Q^2}}{j j} \right]; \quad (7)$$

The two solutions N_{cjd} and s_{cjd} mean that we have two partial aggregation domains. Taking $x = 0$ and $x = 1$ in Eq. (6), we get two outer boundaries

$$s_{cjd}(p; x = 0) = s_{cjd} + pN_{cjd}; \quad (8)$$

and two inner boundaries

$$s_{cjd}(p; x = 1) = s_{cjd} + p[N_{cjd} - (c_s)(N_{cjd} - N_i)] \quad (9)$$

of the partial aggregation domains. The corresponding phase diagram is shown in Fig. 4b. The outer boundaries are also the boundaries of the whole aggregation domain (including partial and total aggregation domains), at which all free macroion-Z⁻ions complexes are still stable ($x = 0$). The inner boundaries are also the boundaries of the total aggregation domain at which there is no free macroion-Z⁻ions complex ($x = 1$). When s increases from zero, first the aggregate forms, then it dissolves. Thus we arrive at a phase diagram of reentrant condensation. According to Eq. (8), the slopes, ds/dp , of the outer boundaries are N_{cjd} , which are the numbers of Z⁻ions in a free macroion-Z⁻ions complex. Since N_{cjd} are solutions to N in the whole partial aggregation domain, the number of Z⁻ions complexed with one free macroion is fixed in the partial aggregation domain. According to Eq. (9), the slopes of the inner boundaries are $N_{cjd} - (N_{cjd} - N_i)$, which are the numbers of Z⁻ions in an aggregated complex. On the other hand, s_{cjd} are the intercepts of these boundaries with p axis. The dashed line on Fig. 4b corresponds to solutions with neutral macroion-Z⁻ions complexes and can be calculated from Eq. (3). Taking $N = N_i$ in this equation, we get

$$s_0(p) = \frac{1}{v_0} \exp \left[\frac{j j}{k_B T} \right] + pN_i; \quad (10)$$

This line has the same slope as the isoelectric line $s_i = pN_i$ (dotted line in Fig. 4), but a small finite intercept. This is because there is always a small fraction of free Z⁻ions in the solution.

When $\alpha = 1$, the whole surface of a macroion in the aggregate is neutral, all formulae above reproduce the corresponding results in the case $r_s = R$ ¹¹. For example, the boundaries of the total aggregation domain given by Eq. (9) are now parallel lines

$$s_{cjd}(p; x = 1) = s_{cjd} + pN_i; \quad (11)$$

The corresponding phase diagram for $r_s = R$ is shown in Fig. 4a.

There are four parameters c , c_s , C and v_0 in the theory. Their values depend on the screening radius r_s , the shape and flexibility of the macroions and Z⁻ions. In the following sections, we calculate them for specific systems. But

even now we can qualitatively summarize the evolution of the phase diagram with decreasing r_s . For this purpose, we define the size of an aggregation domain as the absolute value of the difference of the slopes of its two boundaries. As r_s decreases, (r_s) decreases, $C(r_s)$ increases, while β is fixed (this will be shown below). Then according to Eq. (5), N_d increases and N_c decreases. Thus, both the size of the whole aggregation domain (including partial and total aggregation domains), $N_d + N_c$, and the size of the total aggregation domain, $(1 - \beta)(N_d + N_c)$, grow with decreasing r_s . In contrary to them, the relative size of the two partial aggregation domains in the whole aggregation domain, $(N_d - N_c)/(N_d + N_c) = \beta$, decreases with decreasing r_s .

As we mentioned before, at $r_s < r$ the growth of the aggregation domain and reduction of the relative size of the partial aggregation domain continue with decreasing r_s . In this regime, however, the range of Coulomb interaction and correlation becomes the same and one can not separate these interactions from each other. A microscopic theory is necessary, which operates with screened interaction of Z-ions with macroion and with each other and allows for small dielectric constant of macroion. This is a subject of future work.

III. RIGID SPHERICAL MACROIONS

In this section, we consider the system with spherical macroions and much smaller spherical Z-ions (Figs. 2). We estimate parameters β , C and microscopically and find out how borders of the aggregation domain change with decreasing screening radius r_s .

Let us first consider the case $r_s = R$. In this case, each macroion carries N_i Z-ions in the aggregate and $\beta = 1$. In the first order approximation, Z-ions repel each other to form 2D Wigner crystal on the surface of a macroion. Thus the correlation chemical potential ϕ_c is approximately²¹

$$\phi_c = \frac{1.6Z^2e^2}{Dr}; \quad (12)$$

where r is the radius of the Wigner-Seitz cell when a macroion is neutralized by Z-ions (see Figs. 2) and D is the dielectric constant of water. To calculate β , we first notice that the number of Z-ions in a sticky region is

$$N_i \frac{W^2}{4R^2} = \frac{P N_i}{2}; \quad (13)$$

where relation $N_i = 4R^2 = r^2$ has been used. If each macroion has nearest neighbors in the aggregate ($b = 12$ for dense packing),

$$\beta = \frac{b}{2} \frac{P}{N_i} \phi_c = 0.4b \frac{ZeQ}{DR}; \quad (14)$$

Here we assumed that each Z-ion in the sticky region gains the correlation energy ϕ_c . The maximum possible

can be estimated as follows. Since the surface density of Z-ions is doubled in the contact region, the radius of the Wigner-Seitz cell becomes $r = \frac{R}{\sqrt{2}}$ and the correlation energy per Z-ion gets a factor $\sqrt{2}$. This gives $\beta \approx 0.3$. The real β is much smaller than this upper limit due to the effect of small dielectric constant of macroions. As is well known in electrostatics, positive Z-ions in water ($D \approx 80$) creates positive images in adjacent macroions ($D \approx 80$). Repulsion from images push two contacting macroions away from each other and diminishes the gain of correlation energy. Finally, for a spherical macroion with Z-ions whose size is negligible, the capacitance is

$$C = DR; \quad (15)$$

Using Eqs. (5) and (7), we get

$$N_{c,d} = N_i \left(1 - \frac{P}{0.2b} \frac{r}{R} \right); \quad (16)$$

$$S_{c,d} = \frac{1}{v_0} \exp \left(\frac{1.6Z^2e^2}{k_B T D r} \right) \left(1 - \frac{b}{0.8} \right); \quad (17)$$

Let us now switch to the case $r_s < R$. Since the sticky region is much smaller than the neutral region (see Fig. 7), the short-range correlations are not changed by screening, ϕ_c and β are still given by Eqs. (12) and (14). But C and C are affected by screening. For simplicity, we estimate C by assuming that the whole r_s -cylinder is neutral. Then C reduces to the area ratio of the neutral region to the whole surface of the complex,

$$C = \frac{b \frac{W^2}{4R^2}}{\frac{b r_s}{2R}} = \frac{b r_s}{2R}; \quad (18)$$

And

$$C = \frac{DR^2}{r_s}; \quad (19)$$

This gives

$$N_{c,d} = N_i \left(1 - \frac{P}{0.4} \frac{r}{r_s} \right); \quad (20)$$

$$S_{c,d} = \frac{1}{v_0} \exp \left(\frac{1.6Z^2e^2}{k_B T D r} \right) \left(1 - \frac{r}{0.4 r_s} \right); \quad (21)$$

It is easy to check that in both cases $N_{c,d}$ are close to N_i . This justifies the approximation (2) used in the last section. From Eq. (20), we see that the aggregation domain broadens with decreasing r_s and the angle it occupies becomes the order of unity at $r_s = r$. According to Eq. (18), the relative size of the partial aggregation domain decreases with r_s proportionally to r_s/R .

Two comments on validity of our approach are in order here. First, we assumed above that at $s > s_d(p)$, when overcharged macroions redissolve, they still keep almost all Z-ions. As is well known²¹, the condition of maximum charge inversion is given by

$$\phi_c = \frac{ZeQ}{C}; \quad (22)$$

Denoting N_{max} the maximum number of Z-ions on a macroion, and using Eq. (12), in the case of $r_s = R$ we have

$$N_0 = N_i \left(1 + 0.4 \frac{r}{r_s} \right) \quad (23)$$

Comparing with Eq. (20), we see that N_{max} and N_d are of the same order of magnitude. As we mentioned above we believe that $\alpha < 0.3$ so that $N_d < N_{max}$ and the picture of stable complexes on both sides of aggregation domain is justified.

Second, up to now we discussed screening by monovalent salt in Debye-Huckel approximation. When a Z-ion has large charge and small size a , they are screened nonlinearly. Monovalent counterions condense on Z-ions (similarly to the Manning screening of a charged cylinder) and renormalize the charge of a free Z-ion to a smaller value Z^{022} . The charge Z^0 is screened in Debye-Huckel way. When adsorbed to the macroion surface, Z-ion is subjected to the additional Coulomb interactions with both the negative macroion surface and neighboring Z-ions. Both interaction energies are of the order of $Z^0 e^2 = r$ and at r can be ignored in comparison with with the chemical potential of the monovalent counterion $Z^0 e^2 = a$ on Z-ion. Therefore, the effective charge Z^0 is not changed by Z-ion condensation and should be used as the effective charge of a Z-ion in all our results²³.

In recent Monte Carlo simulations of the system of spherical macroions with multivalent Z-ions²⁴, it is seen that around the isoelectric line $s_i = pN_i$, all macroions aggregate, while far away from this line on both sides, free macroion-Z-ions complexes are stable. This qualitatively agrees with our theory.

IV. CYLINDRICAL MACROIONS

In this section, we consider the system with cylindrical macroions and much smaller spherical Z-ions (Fig. 3). We show that the qualitative feature of the phase diagram of this system is the same as spherical macroions. The major difference is that for cylinders, s_d is much larger.

We assume that charge of the macroion and Z-ion is such that $r = R$. Accordingly two dimensional Wigner-Crystal-like structure of Z-ions can be formed on the surface of macroions¹⁹. We also assume that $r_s < L$. Consequently below we focus on two cases corresponding to $R = r_s = L$ and $R = r_s < R$. Also note that in order to gain more contact area and, therefore, more correlation energy, all cylinders in the aggregate are parallel to each other.

We first consider the case $R = r_s = L$. It is easy to see that the aggregate should be neutral, i.e., $\alpha = 1$, and the chemical potential μ_c is still given by Eq. (12). However, α is not the same since the area of the sticky region is much larger. It is not a disk, but a stripe with

area $2W L$. The number of Z-ions in the sticky region is

$$N_i \frac{2W L}{2 R L} = \frac{1}{2} N_i \frac{r}{R} \quad (24)$$

For a macroion with b nearest neighbors ($b = 6$ for dense packing), the additional correlation energy per macroion is

$$= \frac{b}{2} N_i \frac{r}{R} \quad (25)$$

Here α takes the same value as the one for spherical macroions. And the capacitance is

$$C = \frac{D L}{2 \ln(r_s = R)} \quad (26)$$

Using Eqs. (5) and (7), we have

$$N_{c,d} = N_i \left(1 + \frac{0.8b}{\ln(r_s = R)} \frac{r}{R} \right)^{\frac{3}{4}} \quad (27)$$

$$S_{c,d} = \frac{1}{v_0} \exp \left[\frac{1.6 Z^2 e^2}{k_B T D r} \right] \left(1 + \frac{b}{0.2} \frac{\frac{1}{2}}{\ln \frac{r_s}{R}} \frac{R}{r} \right)^{\frac{1}{4}} A_5 \quad (28)$$

Now we consider the case $r = r_s = R$. Instead of a neutral aggregate, we only require a stripe-like neutral region in the present case. It is easy to see that both α and μ_c are not changed by screening. The fraction of the neutral area is

$$= b \frac{2W_s L}{2 R L} = \frac{b}{2} \frac{r}{R} \quad (29)$$

while the capacitance

$$C = \frac{D R L}{2 r_s} \quad (30)$$

We have

$$N_{c,d} = N_i \left(1 + \frac{0.8}{2} \frac{r}{r_s} \right)^{\frac{3}{4}} \quad (31)$$

$$S_{c,d} = \frac{1}{v_0} \exp \left[\frac{1.6 Z^2 e^2}{k_B T D r} \right] \left(1 + \frac{b}{0.2} \frac{\frac{1}{2}}{2} \frac{r_s}{r} \right)^{\frac{1}{4}} A_5 \quad (32)$$

Again in both cases $N_{c,d}$ are close to N_i and the approximation (2) is valid. According to Eq. (29), the relative size of the partial aggregation domain decreases with r_s proportionally to $r_s = R$. We see that the aggregation domain are wider in the case of cylindrical macroions than that for spherical macroions (see Sec. III). This happens because of the larger contact area in the former case.

According to Eq. (32), formally s_d can be even larger than $1/v_0$. Consequently, one may conclude that the aggregate never dissolves at large s . Actually, this is not true. When s becomes so large that the distance between Z -ions in the bulk is equal to r_s , the repulsion between free Z -ions can not be ignored and our theory is invalid. At such a large concentration, Z -ions are correlated not only on the surface of macroions but also in the bulk and aggregation does not happen. What we can conclude is that for systems discussed in this section, the aggregate dissolves at very large s . Mathematically, s_d is so large that $\ln(1/s_d v_0) \approx \ln(s_d/s_c)$. Correspondingly, the aggregation domain in Fig. 4 at $s > s_i$ is very wide.

The results above can be qualitatively compared with experimental results for solutions of DNA with spermine^{4,5,6,7} in which long DNA double helices may be considered as rigid negative cylinders and short positive spermine molecules as small Z -ions ($Z = 4$). In experiments, reentrant condensation is observed. Also the aggregation domain at small p is very wide ($\log(s_d/s_c) \approx 4$). Both facts agree with our theory.

V. ARTIFICIAL CHROMATIN

In this section, we discuss the artificial chromatin in which macroions are long semi-flexible polymers with linear charge density λ and Z -ions are hard spheres with radius R (Fig. 1). We assume $\lambda R = Ze$, i.e., many turns of polymer segments are needed to neutralize one sphere. The aggregate of such a system looks like Fig. 3 in Ref. 11. The phase diagram of this system has already been discussed in detail in Ref. 11 under the assumption that the aggregate is always neutral which is valid only for $r_s \approx R$. When $r_s \gg R$, there is no justification for the neutrality of the aggregate and the theory in Sec. II should be used. Here we calculate the parameters microscopically and obtain the phase diagram for the later case.

First, let us remind the results following directly from Ref. 11. In this case, each macroion- Z -ions complex carries $N_i Z$ -ions in the aggregate. Correspondingly, $\alpha = 1$. The correlation chemical potential ϕ_c is essentially the self-energy of a bare free sphere in the solution which is almost totally eliminated in the complex. Therefore

$$\phi_c = \frac{Z^2 e^2}{2D R}; \quad (33)$$

where D is the dielectric constant in water solution. To calculate ϕ_c , we first notice that the correlation energy per unit length of the polymer is just the interaction energy of the polymer turn with its stripe of background (sphere) positive charge. Thus, it is $\frac{1}{2} \ln(R/\lambda) = D$. Correspondingly, when the density doubles, λ is halved, the gain in correlation energy per unit length is $\frac{1}{2} \ln 2 = D$, where $\ln 2$ as a rough estimate. Similar to the case of spherical macroion, the radius of the sticky region $W_s \approx R\lambda = 2R$. And the polymer length in this region

is $W_s^2 \lambda = R = 2$. Since each aggregated complex carries $N_i Z$ -ions and has b nearest neighbors, we have

$$C = \frac{b R^2}{2 D} N_i; \quad (34)$$

where $b = 6$ if the maximum packing number is achieved. The capacitance

$$C = \frac{D L}{2 \ln(r_s/R)} = \frac{D R N_i}{\ln(r_s/R)}; \quad (35)$$

where we have used $L \approx 2 R N_i$, because near neutrality, each polymer absorbs about N_i spheres and all spheres in the macroion- Z -ions complex are densely packed. Using Eqs. (5) and (7), we have

$$N_{c,d} = N_i \left(1 - \frac{b R}{\ln(r_s/R)} \right) \frac{1}{Ze}; \quad (36)$$

$$s_{c,d} = \frac{1}{v_0} \exp \left(\frac{Z^2 e^2}{2 k_B T D R} \left(1 - \frac{b R}{\ln(r_s/R)} \right) \right); \quad (37)$$

This gives a typical phase diagram of reentrant condensation (Fig. 4a).

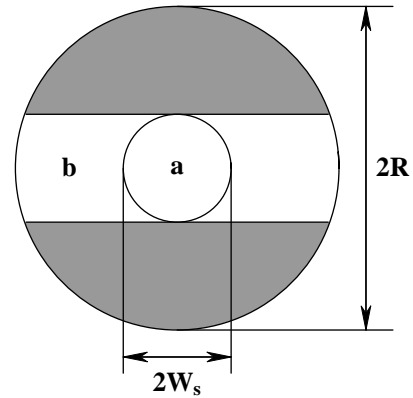


FIG. 8: A 2D view of the surface of a sphere touching the other sphere at the center of the disk-like region a . To make a neutral, a semi-flexible polymer have to change the density of its turns to make the whole equatorial stripe-like region b neutral. The rest of the surface colored in gray is charged.

Now let us consider the case when $\lambda R \approx R$. λ being the average distance between two polymer turns on the surface of spheres when polymer segments exactly neutralize the sphere (see Fig. 1). Since $\lambda R \approx R$, the requirement $\lambda R = R$ is equivalent to $R \approx Ze$. As we discussed in Sec. II, with the screening of monovalent salt, the whole aggregate need not be neutral, but disk-like regions on spheres where two spheres touch each other must be neutral (see Fig. 7). The radius of this region $W_s = \frac{R}{2r_s}$. In the present case, the neutral region should be made by the rearrangement of the polymer segments on the surface of spheres. If the polymer

is extremely flexible, it can bend easily in the disk-like region. By this bending, the surface density of polymer segments is changed "locally" so that the region can be made neutral and the rest of the surface is not changed. However, if the polymer is only semi-flexible (the persistent length l_p is such that $r_s R \ll l_p \ll R$), it is too rigid to neutralize the disk-like region. Then this region can be made neutral only by changing distances between sequential turns of the polymer on the surface of the sphere. For example, for two touching spheres (Fig. 5), the equatorial stripe-like region shown in Fig. 8 can be made neutral. We focus on the case of the semi-flexible polymer which corresponds to DNA.

When $A \approx r_s R$, the correlation chemical potential μ_c is still given by the self-energy of a bare free sphere, which is now

$$\mu_c = \frac{r_s Z^2 e^2}{2D R^2}; \quad (38)$$

and the correlation gain due to aggregation, μ_a , is still given by Eq. (34). This is because the contact region where the additional correlational energy is gained is much smaller than the neutral region as discussed in Sec. II. Also since the number of Z-ions in each complex in the aggregate is close to N_i , in the first order approximation, we can use N_i as the number of Z-ions in each complexes in Eq. (34). Knowing that the area of the strip-like region is $4\pi W_s R$ (see Fig. 8), the area ratio is given by

$$\frac{\mu_a}{\mu_c} = \frac{4\pi W_s R}{4\pi R^2} = \frac{r_s}{R}; \quad (39)$$

And the capacitance is now

$$C = \frac{D R L}{2r_s} = \frac{D R^2}{r_s} N_i; \quad (40)$$

Using Eqs. (5) and (7), we have

$$N_{c;d} = N_i \left[1 - \frac{b}{2} \frac{R}{Z e} \frac{R}{r_s} \right]^{\frac{3}{4}}; \quad (41)$$

$$s_{c;d} = \frac{1}{v_0} \exp \left[-\frac{r_s Z^2 e^2}{2k_B T D R^2} \right] \left[1 - \frac{b}{2} \frac{R}{Z e} \frac{R}{r_s} \right]^{\frac{3}{4}}; \quad (42)$$

The phase diagram is shown in Fig. 4b.

It is easy to check that in both two cases, slopes $N_{c;d}$ are close to N_i and the approximation (2) is valid. Comparing $s_{c;d}$ and $N_{c;d}$ with results for spherical and cylindrical macroions, we see that aggregation domain of the artificial chromatin is the smallest of all three cases if parameter $R = Z e$ is small (the polymer makes many turns around the sphere). The main reason is that in artificial chromatin, μ_c and μ_a originate from two different kinds of correlations. At $R = Z e$, the correlation energy of two polymer turns of the touching sphere is much smaller

than the correlation energy of the sphere in the complex (it interacts with all turns of the polymer).

An artificial chromatin system in the presence of monovalent salt is studied in experiments²⁰, where the phase diagram of reentrant condensation is found and the domain of partial aggregation is not observed. This is qualitatively consistent with our theory that the relative size of the partial aggregation domain is small due to screening effect of monovalent salt.

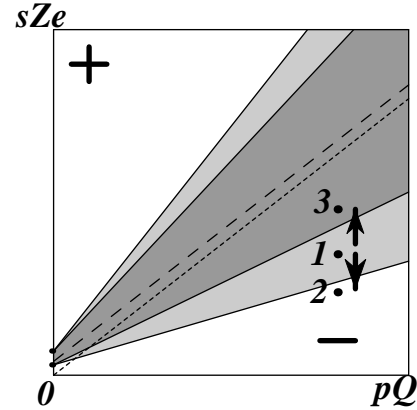


FIG. 9: The chromatin regulation and compaction. sZe is the concentration of charge of histones, pQ is the concentration of DNA. All lines and charges have the same meaning as in Fig. 4. Normal chromatin is at the point 1. A acetylation of histones, moves it to the point 2 (downward arrow). On the other hand, addition of protamines during spermatogenesis compacts chromatin into the more condensed state 3 (upward arrow).

The phase diagram Fig. 4b may be useful for qualitative understanding of chromatin regulation. It is known¹ that chromatin can switch from the compact state of 30 nm fiber or higher order structures to the loose state of 10 nm fiber in which gene transcription takes place. This transition is caused by acetylation of core histones, which reduces the number of positive charges of histone octamers. Experiments *in vitro*¹⁵ show that the transition happens when the charge of the octamer $Z e$ (about $+160e$ in normal conditions) is reduced by $+12e$, i.e., only by 8%. Such a sensitive response can be understood in our theory as shown in the phase diagram Fig. 9 in the plane of total charges of octamers and DNA. Normal chromatin seems to be partially aggregated and the system is at state 1. Under acetylation, the charge of octamers is reduced so that the system moves down to state 2 below the partial aggregation domain. The small partial aggregation domain is crucial for the sensitive response. Fig. 9 also helps to understand spermatogenesis in which normal chromatin is compacted further by adding strongly positively charged proteins, protamines¹. In the solution, the concentration of the positive charge increases and the system moves up from state 1 to state 3 in the total aggregation domain.

To conclude this section, let us make a comment about the role of Manning condensation of monovalent salt on DNA. Above we literally dealt with the case when the linear charge density of the polymer is smaller than critical density $\rho_c = k_B T / e$ of Manning condensation. As is well known, for a free polymer with $\rho > \rho_c$ (for example, for DNA double helix, which has $\rho = 4.2 \rho_c$), is renormalized to ρ_c . For DNA wrapping a positive sphere in artificial chromatin, this renormalization is different because of the surface charge of positive spheres. Such renormalization and its consequence on the phase diagram were studied in Ref. 11.

VI. CONCLUSION

In this paper we developed a phenomenological theory of complexation and aggregation in asymmetric water solutions of strongly charged negative and smaller positive colloids (macroions and Z-ions) in the presence of a large concentration of monovalent salt. We showed that in contrary with earlier theory¹¹ mostly devised for salt free solutions, aggregate of complexes can carry net charge of macroions and Z-ions which is almost as large

as the charge of free complexes. Only small touching regions of each aggregated complex are depleted of the net charge. As a result screening by monovalent salt leads to broader aggregation domain in the phase diagram of the solution and to narrower, but still finite domain of partial aggregation where aggregate is in equilibrium with free complexes. Our phenomenological theory expressed properties of the phase diagram through several parameters which depend on charges of macroions and Z-ions, their sizes, shapes, flexibility and screening of monovalent salt. For three different pairs of macroions and Z-ions we evaluated these parameters and discussed differences and trends in their phase diagrams. We found out that one of these systems, which we call artificial chromatin (see Fig. 1), indeed has phase diagram qualitatively similar to the one of natural chromatin.

Acknowledgments

The authors are grateful to S. G. Rigoryev, A. Yu. Grosberg, V. Lobaskin, T. T. Nguyen, and E. Raspaud for useful discussions. This work is supported by NSF No. DMR-9985785 and DMI-0210844.

- ¹ B. Alberts, A. Johnson, J. Lewis, M. Raff, K. Roberts, and P. Walter, *Molecular Biology of the Cell* (Galland, New York, 2002).
- ² J. Widom, *J. Mol. Biol.*, **190**, 411 (1986).
- ³ V. A. Bloomfield, C. Ma, and P. G. Arscoot, *ACS Symp. Ser.*, **548**, 185 (1994).
- ⁴ J. Pelta, F. Livolant, and J.-L. Sikorav, *J. Biol. Chem.*, **271**, 5656 (1996).
- ⁵ E. Raspaud, M. Olivera de la Cruz, J.-L. Sikorav, and F. Livolant, *Biophysical Journal*, **74**, 381 (1998).
- ⁶ E. Raspaud, I. Chaperon, A. Leforestier, and F. Livolant, *Biophysical Journal*, **77**, 1547 (1999).
- ⁷ M. Saminathan, T. Antony, A. Shirahata, L. H. Sigal, T. Thomas, and T. J. Thomas, *Biochemistry*, **38**, 3821 (1999).
- ⁸ E. Lai and J. H. van Zanten, *Biophysical Journal*, **80**, 864 (2001).
- ⁹ E. Lai and J. H. van Zanten, *Journal of Controlled Release*, **82**, 149 (2002).
- ¹⁰ H. W. W. alker and S. B. G rant, *Colloids and Surfaces A*, **119**, 229 (1996) and reference therein.
- ¹¹ T. T. Nguyen and B. I. Shklovskii, *J. Chem. Phys.*, **115**, 7298 (2001).
- ¹² This behavior is different from the one resulting from the assumption that for a given (p, s) all macroion-Z-ions complexes have same charge. Such assumption would lead to a picture of aggregate as an uniformly charged liquid of complexes. According to the classical Rayleigh theory¹³ of instability of a charged liquid, this liquid would form droplets with the size optimizing the sum of their surface and charging energy (see also Ref. 14 and references therein). Possibility to redistribute Z-ions between complexes makes the system more flexible and leads to a deeper minimum of the total free energy.
- ¹³ Rayleigh, *Lord Philos. Mag.*, **14**, 184 (1882).
- ¹⁴ A. V. Dobrynin, M. Rubinstein, and S. P. Obukhov, *Macromolecules*, **29**, 2974 (1996).
- ¹⁵ C. T. S. T. Sera, A. P. Wolle, and J. C. Hansen, *Mol. Cell biology*, **18**, 4629 (1998).
- ¹⁶ I. Rouzina and V. A. Bloomfield, *J. Phys. Chem.*, **100**, 9977 (1996).
- ¹⁷ I. M. Ruzin, S. Marianer, and B. I. Shklovskii, *Phys. Rev. B*, **46**, 3999 (1992).
- ¹⁸ The definition of ϵ is different from Ref. 11. There notation " ϵ " is used to define the additional correlation energy per Z-ion in the aggregate. The definition used here is more convenient for systems shown Fig. 2 and Fig. 3 in which not all Z-ions in the aggregate can gain the additional correlation energy.
- ¹⁹ B. I. Shklovskii, *Phys. Rev. Lett.*, **82**, 3268 (1999).
- ²⁰ K. Keren, Y. Soen, G. Ben Yoseph, R. Gilad, E. Braun, U. Sivan, and Y. Talmon, *Phys. Rev. Lett.*, **89**, 088103 (2002).
- ²¹ A. Yu. Grosberg, T. T. Nguyen, and B. I. Shklovskii, *Rev. Mod. Phys.*, **74**, 329 (2002).
- ²² M. Gueron and G. W. Eisebich, *Biopolymers*, **19**, 353 (1980); S. Alexander, P. M. Chaikin, P. Grant, G. J. Morales, P. Pincus, and D. Hone, *J. Chem. Phys.*, **80**, 5776 (1984); S. A. Safran, P. A. Pincus, M. E. Cates, and F. C. MacKintosh, *J. Phys. (France)*, **51**, 503 (1990).
- ²³ T. T. Nguyen, A. Yu. Grosberg and B. I. Shklovskii, *J. Chem. Phys.*, **113**, 1110 (2000).
- ²⁴ P. Linse and V. Lobaskin, *Phys. Rev. Lett.*, **83**, 4208 (1999); V. Lobaskin and K. Qamhieh, *cond-mat/0212182*.